

REPORT No. 871

DETERMINATION OF ELASTIC STRESSES IN GAS-TURBINE DISKS

By S. S. MANSON

SUMMARY

A method is presented for the calculation of elastic stresses in symmetrical disks typical of those of a high-temperature gas turbine. The method is essentially a finite-difference solution of the equilibrium and compatibility equations for elastic stresses in a symmetrical disk. Account can be taken of point-to-point variations in disk thickness, in temperature, in elastic modulus, in coefficient of thermal expansion, in material density, and in Poisson's ratio. No numerical integration or trial-and-error procedures are involved and the computations can be performed in rapid and routine fashion by nontechnical computers with little engineering supervision. Checks on problems for which exact mathematical solutions are known indicate that the method yields results of high accuracy.

Illustrative examples are presented to show the manner of treating solid disks, disks with central holes, and disks constructed either of a single material or of two or more welded materials. The effect of shrink fitting is taken into account by a very simple device.

INTRODUCTION

One of the problems in the design of gas turbines is the determination of the stresses in the turbine disk under operating conditions. Calculation of the elastic-stress distribution is a first step in the determination of the true stress distribution. This stress distribution is based on the assumption of linearity of stress with strain and differs from the true stress distributions, which may contain stresses beyond the proportional elastic limit of the material.

The equations for the elastic-stress distribution in symmetrical disks are well known. Their solution may, however, offer considerable difficulty. One difficulty encountered in calculation of the operating stresses in disks with high-temperature gradients is that the physical properties of the materials, such as elastic modulus, Poisson's ratio, and coefficient of thermal expansion, vary with the temperature and therefore have a different value at each location in the disk. In addition, the thickness of the turbine disk varies from radius to radius. If the disk consists of portions of different materials welded to each other, the density may vary from one section to the other. Shrink fitting and welding of the component parts at elevated temperatures also introduce special stress problems. Attempts to find complete analytical solutions for the stress problems that take into

account shrink fitting and point-to-point variation of the physical properties and of the disk thickness result in mathematical complexities; approximate solutions are therefore usually found by numerical methods.

Thompson in reference 1 gives a numerical approach to the turbine-disk problem that takes into account point-to-point variation in disk thickness and in all physical properties except Poisson's ratio. A method capable of easily accounting for shrink fitting and for the variation in Poisson's ratio as well as in the other properties was developed in 1945 at the NACA Cleveland laboratory and is presented in the analytical section herein. The method is essentially a finite-difference solution of the differential equations of stress in a rotating disk and incorporates several advantageous features uncommon to other forms of solution. For example, numerical integration and trial-and-error processes have been completely avoided, which makes it possible for nontechnical computers to carry through the entire solution rapidly and with little engineering supervision.

In the second section of this report, illustrative examples are presented to show the manner of treating a solid disk and a disk with a central hole for application to a gas turbine. The examples are self-explanatory and may be used as a guide for the solution of turbine-disk problems without reference to the analytical section of the report in which the basis for the solution is derived.

The method also has applicability to the study of stresses in rotating disks other than that in the gas turbine. It has been applied, for example, to disks of axial-flow compressors in which the only complicating factor is variable disk thickness. For such application the main advantages of the method are the routine nature of the calculation, the rapidity with which the calculations can be made, and the accuracy of the final results.

ANALYSIS

SYMBOLS

The following symbols are used:

A	point midway between n th and $(n-1)$ st point stations
E	elastic modulus of disk material, (lb/sq in.)
h	axial thickness of disk, (in.)
r	radial distance, (in.)
u	radial displacement of any point on disk as disk passes from unstressed to stressed condition

- α coefficient of thermal expansion between actual temperature and temperature at which there is zero thermal stress, (in./in.)(°F)
- ΔT temperature increment above that at which there is zero thermal stress
- ϵ_r radial strain, (in./in.)
- ϵ_t tangential strain, (in./in.)
- μ Poisson's ratio
- ρ mass density of disk material, ((lb)(sec²)/in.⁴)
- σ_r radial stress, (lb/sq in.)
- σ_t tangential stress, (lb/sq in.)
- ω angular velocity of disk, (radians/sec)

The following supplementary subscripts are used for denoting values of the preceding symbols in connection with the finite-difference solution:

- n n th point station
- $n-1$ $(n-1)$ st point station
- a station at the smallest radius of the disk considered (For a disk with a central hole, this station is taken at the radius of the central hole; for a solid disk, this station is taken at a radius of about 5 percent of rim radius.)

b rim of disk or base of blades

Example of the use of double subscript:

$\sigma_{r,n-1}$ radial stress σ_r at station $n-1$

The following supplementary symbols denote combinations of the foregoing symbols arising in the analysis:

$A_{r,n}$ } coefficients defined by equations
 $A_{t,n}$ }
 $B_{r,n}$ }
 $B_{t,n}$ }

$$C_n = r_n h_n$$

$$C'_n = \frac{\mu_n}{E_n} + \frac{(1+\mu_n)(r_n - r_{n-1})}{2E_n r_n}$$

$$D_n = \frac{1}{2} (r_n - r_{n-1}) h_{n-1}$$

$$D'_n = \frac{1}{E_n} + \frac{(1+\mu_n)(r_n - r_{n-1})}{2E_n r_n}$$

$$F_n = r_{n-1} h_{n-1}$$

$$F'_n = \frac{\mu_{n-1}}{E_{n-1}} - \frac{(1+\mu_{n-1})(r_n - r_{n-1})}{2E_{n-1} r_{n-1}}$$

$$G_n = \frac{1}{2} (r_n - r_{n-1}) h_{n-1}$$

$$G'_n = \frac{1}{E_{n-1}} - \frac{(1+\mu_{n-1})(r_n - r_{n-1})}{2E_{n-1} r_{n-1}}$$

$$H_n = \frac{1}{2} \omega^2 (r_n - r_{n-1}) (\rho_n h_n r_n^2 + \rho_{n-1} h_{n-1} r_{n-1}^2)$$

$$H'_n = \alpha_n \Delta T_n - \alpha_{n-1} \Delta T_{n-1}$$

$$K_n = \frac{F'_n D_n - F_n D'_n}{C'_n D_n - C_n D'_n}$$

$$K'_n = \frac{C_n F'_n - C'_n F_n}{C'_n D_n - C_n D'_n}$$

$$L_n = -\frac{G'_n D_n + G_n D'_n}{C'_n D_n - C_n D'_n}$$

$$L'_n = -\frac{C'_n G_n + C_n G'_n}{C'_n D_n - C_n D'_n}$$

$$M_n = \frac{H'_n D_n + H_n D'_n}{C'_n D_n - C_n D'_n}$$

$$M'_n = \frac{C'_n H_n + C_n H'_n}{C'_n D_n - C_n D'_n}$$

ASSUMPTIONS

The assumptions are made that stress is proportional to strain and that the disk material is completely elastic at the stress distribution induced by the centrifugal and thermal effects. All variables of material properties and operating conditions are assumed to be symmetrical about the axis of rotation. Axial stresses are neglected and at any radius the radial and tangential stresses are assumed to be uniform across the thickness of the disk. Temperatures are taken in the central plane perpendicular to the axis of the disk.

OUTLINE OF METHOD

In a thin rotating disk of variable thickness, the state of stress at any radius can be completely defined by the two principal stresses, the radial and tangential stresses σ_r and σ_t , respectively. Two equations are therefore necessary to determine the two unknown stresses. The first of these equations can be obtained from the conditions of equilibrium of an element of the disk; the second, from the compatibility conditions, which are mathematical statements of the interrelation between the radial and tangential strains in a symmetrical disk.

The equilibrium and compatibility equations result in differential form defining relations between the stresses at radius r and those at a radius infinitesimally removed from r . Except for some special cases, the solutions of these equations are difficult to obtain. In order to facilitate solution, the differential equations are rewritten in finite-difference form relating the stresses at radius r with those at a radius finitely removed from r . By means of the finite-difference equations, the stresses at an arbitrary finite number of stations along the disk radius are expressed in terms of the stresses at a single reference station near the center of the disk. For a disk with a central hole the reference station is chosen at the inside radius, where the radial stress is zero; hence, the stresses at all stations in the disk are expressed in terms of the single unknown, the tangential stress at this station. For a solid disk, the reference station is chosen at a point near the center of the disk (at a radius of about 5 percent of the disk radius). In this region the radial and tangential stresses can be assumed to be approximately equal; again, therefore, the stresses at all stations are expressed in terms of a single unknown. The unknown can then be determined by the boundary conditions at the rim of the disk where the radial stress is equal to the centrifugal blade loading. When the radial stress at the rim, expressed in terms of the tangential stress at the reference station, is equated to the blade loading, the tangential stress at the reference station is evaluated. After the tangential stress at the reference station has been determined, all the other stresses, expressed in terms of this stress, can be evaluated.

DIFFERENTIAL EQUATIONS

The equilibrium equation, as given in reference 2 (p. 374), using the notation of this paper, is

$$\frac{d}{dr}(rh\sigma_r) - h\sigma_t + \rho\omega^2 hr^2 = 0 \quad (1)$$

The compatibility relation is obtained by elimination of u from the stress-strain displacement equations

$$\epsilon_r = \frac{du}{dr} = \frac{\sigma_r - \mu\sigma_t}{E} + \alpha\Delta T \quad (2)$$

$$\epsilon_t = \frac{u}{r} = \frac{\sigma_t - \mu\sigma_r}{E} + \alpha\Delta T \quad (3)$$

Equation (3) is subtracted from equation (2) to eliminate u ,

$$\frac{du}{dr} - \frac{u}{r} = \frac{(1+\mu)(\sigma_r - \sigma_t)}{E} \quad (4)$$

or

$$\frac{rdu - udr}{r^2} = \frac{(1+\mu)(\sigma_r - \sigma_t)}{E} \quad (5)$$

But

$$\frac{rdu - udr}{r^2} = \frac{d}{dr}\left(\frac{u}{r}\right) \quad (6)$$

Therefore, by equations (3), (5), and (6),

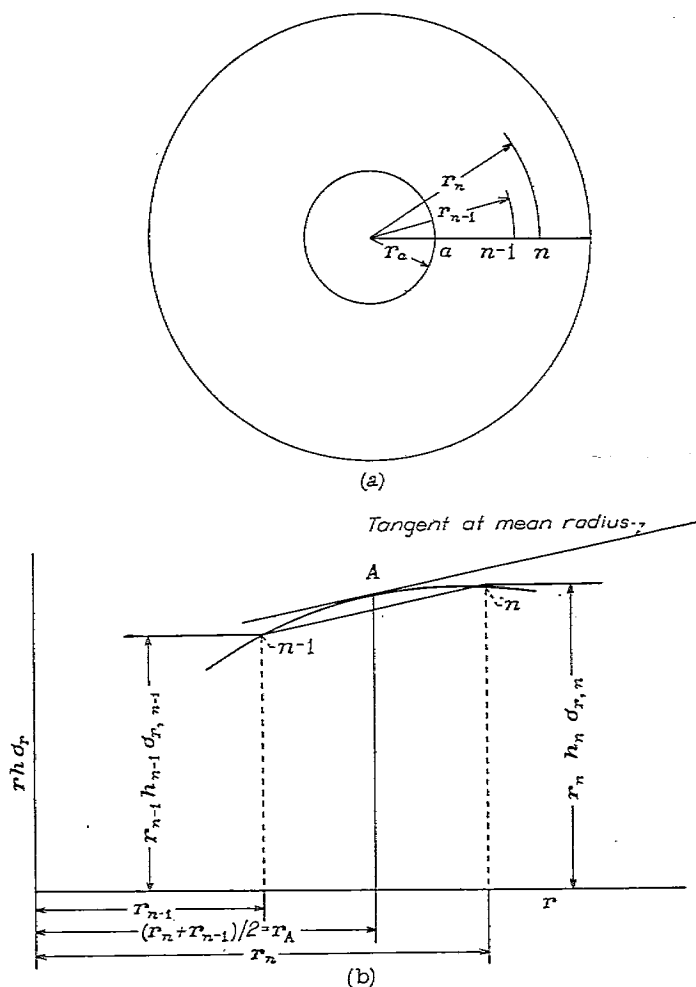
$$\frac{d}{dr}\left(\frac{\sigma_t}{E}\right) - \frac{d}{dr}\left(\frac{\mu\sigma_r}{E}\right) + \frac{d}{dr}(\alpha\Delta T) - \frac{(1+\mu)(\sigma_r - \sigma_t)}{Er} = 0 \quad (7)$$

Equations (1) and (7), together with a knowledge of the boundary conditions, are sufficient to solve for the two unknowns σ_r and σ_t . Because ρ , E , μ , α , ΔT , and h are, in general, functions of the radius r , the equations cannot readily be solved in their differential form; a finite-difference solution was therefore derived.

FINITE-DIFFERENCE EQUATIONS

The translation of differential equations into finite-difference form to facilitate solution is common in engineering practice. The method has, in fact, been applied in limited fashion to the solution of the steam-turbine disk problem (reference 2, pp. 398-400). This application neglects, however, the point-to-point variation in physical properties, and therefore no application to the gas-turbine disk, in which there is appreciable variation in properties from hub to rim, is made. In addition, the solution of the equations involves an interpolation procedure, the elimination of which could considerably reduce the amount of calculation necessary for a solution and increase the accuracy of the final results.

A number of discrete point stations are chosen along the disk radius as shown in figure 1 (a). If it is assumed that the stress distribution in the disk has already been determined, all quantities appearing in equations (1) and (7) are known at each of the point stations and the values of corresponding quantities at the point A midway between the n th and $(n-1)$ st point stations can be approximately determined. For



(a) Location of point stations.
(b) Value of typical function midway between point stations n and $n-1$.

FIGURE 1.—Sketches used to derive finite-difference equations for stresses in symmetrical rotating disk.

example, in the plot of $rh\sigma_r$ against r (fig. 1 (b)), the radius at point A is expressed as

$$r_A = \frac{1}{2}(r_{n-1} + r_n)$$

the value of $rh\sigma_r$ is

$$(rh\sigma_r)_A \approx \frac{1}{2}(r_{n-1}h_{n-1}\sigma_{r,n-1} + r_nh_n\sigma_{r,n})$$

and the slope of the curve at point A , which is approximately equal to the slope of the chord joining points n and $n-1$, is defined as

$$\frac{d}{dr}(rh\sigma_r)_A \approx \frac{r_nh_n\sigma_{r,n} - r_{n-1}h_{n-1}\sigma_{r,n-1}}{r_n - r_{n-1}}$$

In a similar way, the values of each of the other variables entering into the equations can be evaluated for point A . If the evaluations are correct, the quantities at A must satisfy equations (1) and (7). These equations therefore become, in finite-difference form

$$\frac{r_nh_n\sigma_{r,n} - r_{n-1}h_{n-1}\sigma_{r,n-1}}{r_n - r_{n-1}} - \frac{h_n\sigma_{t,n} + h_{n-1}\sigma_{t,n-1}}{2} + \frac{\omega^2}{2}(\rho_nh_nr_n^2 + \rho_{n-1}h_{n-1}r_{n-1}^2) = 0 \quad (8)$$

and

$$\frac{\frac{\sigma_{t,n} - \sigma_{t,n-1}}{E_n} - \frac{\mu_n \sigma_{r,n} - \mu_{n-1} \sigma_{r,n-1}}{E_n}}{r_n - r_{n-1}} + \frac{\alpha_n \Delta T_n - \alpha_{n-1} \Delta T_{n-1}}{r_n - r_{n-1}} - \frac{1}{2} \left[\frac{(1 + \mu_n)(\sigma_{r,n} - \sigma_{t,n})}{E_n r_n} + \frac{(1 + \mu_{n-1})(\sigma_{r,n-1} - \sigma_{t,n-1})}{E_{n-1} r_{n-1}} \right] = 0 \quad (9)$$

which reduce to

$$C_n \sigma_{r,n} - D_n \sigma_{t,n} = F_n \sigma_{r,n-1} + G_n \sigma_{t,n-1} - H_n \quad (10)$$

and

$$C'_n \sigma_{r,n} - D'_n \sigma_{t,n} = F'_n \sigma_{r,n-1} + G'_n \sigma_{t,n-1} + H'_n \quad (11)$$

SOLUTION OF FINITE-DIFFERENCE EQUATIONS

Equations (10) and (11) represent two equations from which $\sigma_{r,n}$ and $\sigma_{t,n}$ can be expressed in terms of $\sigma_{r,n-1}$ and $\sigma_{t,n-1}$. If the linear nature of the equations and the possibility of successive application of the equations to proceed from one station to the next are considered, the stresses at any station can ultimately be expressed in linear terms of the stresses at any other station. It will be convenient to express the stresses at all stations in terms of the stresses at the station a . At this station, the unknown value is the tangential stress $\sigma_{t,a}$; hence, the stresses at station n are expressed in the linear terms

$$\begin{aligned} \sigma_{r,n} &= A_{r,n} \sigma_{t,a} + B_{r,n} \\ \sigma_{t,n} &= A_{t,n} \sigma_{t,a} + B_{t,n} \end{aligned} \quad (12a)$$

and those at station $n-1$ in the form

$$\begin{aligned} \sigma_{r,n-1} &= A_{r,n-1} \sigma_{t,a} + B_{r,n-1} \\ \sigma_{t,n-1} &= A_{t,n-1} \sigma_{t,a} + B_{t,n-1} \end{aligned} \quad (12b)$$

where the coefficients $A_{r,n}$, $B_{r,n}$, $A_{t,n}$, and $B_{t,n}$ are as yet to be determined.

The substitution of equations (12a) and (12b) into equations (10) and (11) and the separation of the terms with and without $\sigma_{t,a}$ result in the equations

$$\begin{aligned} (C_n A_{r,n} - D_n A_{t,n} - F_n A_{r,n-1} - G_n A_{t,n-1}) \sigma_{t,a} + \\ (C_n B_{r,n} - D_n B_{t,n} - F_n B_{r,n-1} - G_n B_{t,n-1} + H_n) = 0 \end{aligned} \quad (13)$$

and

$$\begin{aligned} (C'_n A_{r,n} - D'_n A_{t,n} - F'_n A_{r,n-1} + G'_n A_{t,n-1}) \sigma_{t,a} + \\ (C'_n B_{r,n} - D'_n B_{t,n} - F'_n B_{r,n-1} + G'_n B_{t,n-1} - H'_n) = 0 \end{aligned} \quad (14)$$

The stress $\sigma_{t,a}$ is really arbitrary as far as equations (13) and (14) are concerned because it depends upon the boundary conditions and not on the equations of elasticity from which equations (13) and (14) were derived; that is, by a suitable choice of the factors that determine boundary conditions, such as blade loading and shrink fit, $\sigma_{t,a}$ can be set at any desired value without invalidating in any way the equations

of elasticity (1) and (7), or their ultimate finite-difference forms in equations (13) and (14). If an equation in the form $cx + d = 0$ is to be true for all values of x , the coefficients c and d both must be zero. Because equations (13) and (14) are to be true, independent of the value of $\sigma_{t,a}$, the coefficients of $\sigma_{t,a}$ must be zero, and the two equations reduce to

$$\left. \begin{aligned} C_n A_{r,n} - D_n A_{t,n} - F_n A_{r,n-1} - G_n A_{t,n-1} &= 0 \\ C'_n A_{r,n} - D'_n A_{t,n} - F'_n A_{r,n-1} + G'_n A_{t,n-1} &= 0 \\ C_n B_{r,n} - D_n B_{t,n} - F_n B_{r,n-1} - G_n B_{t,n-1} + H_n &= 0 \\ C'_n B_{r,n} - D'_n B_{t,n} - F'_n B_{r,n-1} + G'_n B_{t,n-1} - H'_n &= 0 \end{aligned} \right\} \quad (15)$$

from which $A_{r,n}$, $A_{t,n}$, $B_{r,n}$, and $B_{t,n}$ can be determined in the form

$$\left. \begin{aligned} A_{r,n} &= K_n A_{r,n-1} + L_n A_{t,n-1} \\ A_{t,n} &= K'_n A_{r,n-1} + L'_n A_{t,n-1} \\ B_{r,n} &= K_n B_{r,n-1} + L_n B_{t,n-1} + M_n \\ B_{t,n} &= K'_n B_{r,n-1} + L'_n B_{t,n-1} + M'_n \end{aligned} \right\} \quad (16)$$

If the coefficients $A_{r,n}$, $A_{t,n}$, $B_{r,n}$, and $B_{t,n}$ are known for station $n-1$, they can be determined by means of equation (16) for station n .

The coefficients at the first station ($r=a$) can be determined by inspection for both the solid disk and the disk with a central hole. Inspection of equation (12a) shows that for a solid disk in which both the tangential and radial stresses at the first station are equal to $\sigma_{t,a}$

$$\begin{aligned} A_{r,a} &= A_{t,a} = 1 \\ B_{r,a} &= B_{t,a} = 0 \end{aligned}$$

For a disk with a central hole in which the radial stress at the first station is zero and the tangential stress is $\sigma_{t,a}$

$$\begin{aligned} A_{r,a} &= B_{r,a} = B_{t,a} = 0 \\ A_{t,a} &= 1 \end{aligned}$$

From these known coefficients at the first station, the coefficients at all other stations can be determined by successive applications of equation (16). Once all the coefficients have been determined, the unknown $\sigma_{t,a}$ can be determined. The radial stress at the rim $\sigma_{r,b}$ is the centrifugal loading of the blades

$$\sigma_{r,b} = A_{r,b} \sigma_{t,a} + B_{r,b}$$

or

$$\sigma_{t,a} = \frac{\sigma_{r,b} - B_{r,b}}{A_{r,b}} \quad (17)$$

where $A_{r,b}$ and $B_{r,b}$ are the coefficients for radial stress at the rim. The radial and tangential stresses at all stations can be obtained from equation (12a) after $\sigma_{t,a}$ and all the coefficients have been determined.

ILLUSTRATIVE APPLICATIONS

CASE I—ELASTIC-STRESS DISTRIBUTION IN SOLID DISK

The profile of a disk that is to be analyzed for stress distribution at a speed of 11,500 rpm and the temperature

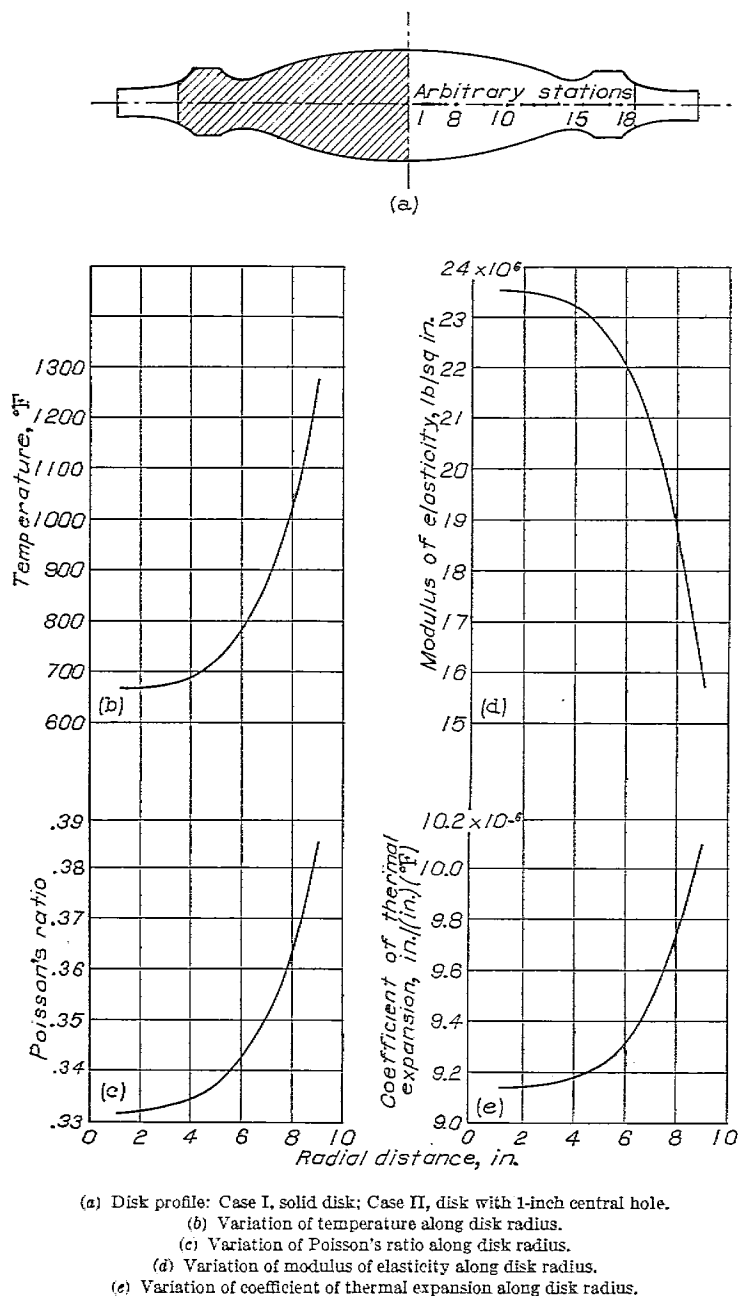


FIGURE 2.—Disk profile, temperature distribution, and variation of physical properties of disk material as function of radius, for illustrative problems.

distribution of the disk are shown in figures 2 (a) and 2 (b), respectively. The first step in the analysis is to choose an arbitrary number of stations along the disk radius. The first station is chosen at a radius of about 5 percent of the rim radius, the last at the rim. The stations need not be equidistant; in fact, it is advisable to choose the stations closely together where there is sharp change in disk contour, in temperature gradient, or in variation of physical properties. In this case 18 stations were chosen, spaced relatively

close together near the rim where the gradients in temperature and physical properties were high and near the center for subsequent use of the same example to illustrate the effect of a central hole. When only a solid disk is considered, no concentration of points near the center is necessary. The various steps of the calculation are tabulated in table I.

The disk radius at each station is listed in column 1 of table I. The thickness of the disk at each station is listed in column 2. A sharp discontinuity in thickness, such as an abrupt flange, should be faired in the disk contour and the faired disk used in determining thickness.

Ordinarily the density of the material is constant throughout the disk, even over the wide range of temperatures. If a faired disk has been used, however, the density of the material in the faired region should be adjusted to produce the total mass that actually exists in the region of each station. Although a flange does not reduce the stress at its own region by increasing the area, its mass must be included as it produces centrifugal stresses throughout the disk. The corrected density at each station multiplied by the square of the rotational speed is listed in column 3. In this case no fairing was necessary; hence, all values of density are equal.

Poisson's ratio, listed in column 4, has only an insignificant effect on the stress distribution and, because no accurate data are available, a constant value of 0.333 may be used. If accurate data on the variation with temperature of Poisson's ratio are available, use of the exact variable values presents no greater difficulty than use of a constant value. The values of μ used in this example are shown in figure 2 (c), and were for convenience obtained by the assumption of a linear variation in μ with temperature.

The modulus of elasticity at each station is listed in column 5. Variations in this property have a significant effect on the final stress values and accurate data should be used if available. For this example, E was arbitrarily assumed to depend linearly upon the temperature, and the variation along the radius is shown in figure 2 (d). In practical computations, the true values of elastic modulus associated with the particular temperature at each station may be used.

The coefficients of thermal expansion are tabulated in column 6. These coefficients must be the average values applicable to the range between the temperatures actually existing and those at which there is no thermal stress. For a homogeneous disk in which there is no shrink fitting of one part to another, the condition of zero thermal stress is at room temperature. Engineering tables usually list the average temperature coefficient of expansion between room temperature and values of high temperature; the listed values may therefore be used directly.

The difference between the actual temperature and the temperature at which there is no thermal stress is listed in column 7. In this case, the stress-free condition is at a room temperature of 70°F . Column 7 is therefore obtained by subtracting 70°F from each of the values in figure 2 (b). This column is of great significance in the case involving shrink fits.

The quantities C_n to M'_n are computed for each station as indicated in columns 8 to 34 of table I. Values in each of these columns can be obtained in one set of operations on a standard computing machine. The method of obtaining the data from the suitable previous columns is indicated at the heading of each column.

Values in columns 33 and 34 must be simultaneously computed. The first value for each of these columns is unity. Subsequent values make use of the previously obtained values in the same columns. Thus, to determine the value for column 33 at station 2, column 27 at station 2 is multiplied by column 33 at station 1, and the product is added to the product of column 28 at station 2 by column 34 at station 1. For example:

$$0.81902 \times 1.0 + 0.18098 \times 1.0 = 1.00000$$

Columns 35 and 36 are likewise simultaneously computed. The first value in each of these columns is zero and each subsequent value is obtained from the previous values in accordance with the symbolic notation given at the head of each column. Thus, to obtain the column 35 at station 2, column 27 at station 2 is multiplied by column 35 at station 1, column 28 at station 2 is multiplied by column 36 at station 1, and the two products are then added to column 31 at station 2

$$0.81902 \times 0 + 0.18098 \times 0 - 67.192 = -67.192$$

Column 37 is uniform for all stations and is obtained from the expression

$$\frac{\sigma_{r,b} - (35)_b}{(33)_b}$$

where $\sigma_{r,b}$ is the blade loading at the rim. The blade loading is obtained by dividing the total centrifugal force at the root of the blades by the total rim peripheral area. In this problem $\sigma_{r,b}$ is 8500 pounds per square inch; column 37 is therefore,

$$\frac{8500 - (-72.896)}{1.93765} = 42,008 \text{ pounds per square inch}$$

Columns 38 and 39 give the radial and tangential stresses, respectively, at each of the stations. As indicated in table I, they are obtained by routine multiplications and additions of columns 33 to 37.

The radial and tangential stresses from columns 38 and 39 are plotted in figure 3. The stresses at the center of the disk are taken equal to those at station a , which is $\frac{1}{2}$ inch removed from the center.

Because the method presented is the only one known to the author that takes into account point-to-point variation in Poisson's ratio, the error involved in the assumption of a constant value of this quantity as compared with the rigorous treatment of its point-to-point variations is valuable to determine. The broken-line curves in figure 3 show calculations for constant values of $\mu = 0.3$ and $\mu = 0.5$ compared with the solid curves, which show the stresses for a contin-

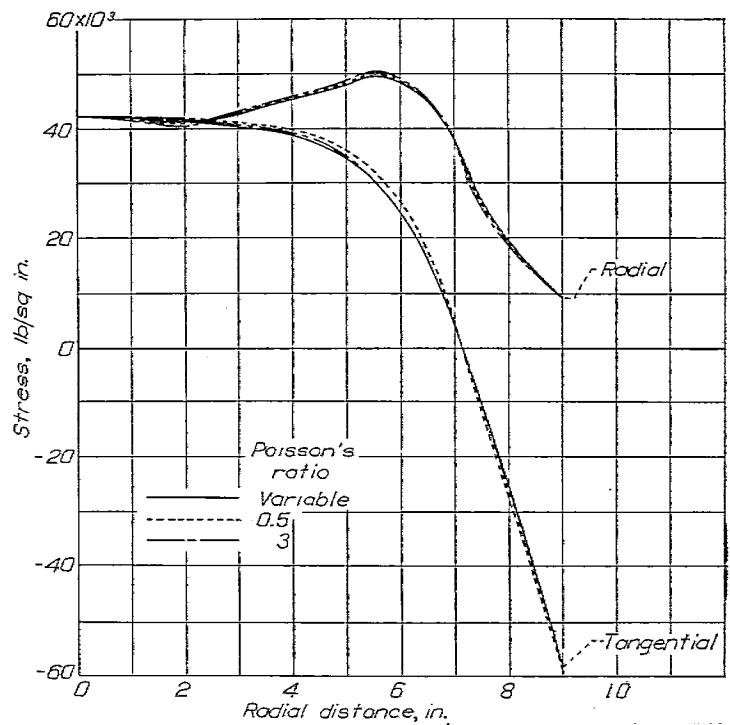


FIGURE 3.—Stress distribution in solid disk of figure 2 computed with constant and with variable values of Poisson's ratio.

uously variable value of μ with temperature, as shown in figure 2 and tabulated in column 4 of table I. The near coincidence of these curves indicates that the assumption of a constant value of μ within the range of actual values results in accurate final values of radial and tangential stresses.

The effect that difference in the number of stations has on the accuracy of the results is shown in figure 4. Little accuracy is gained by the use of additional points; as few as six points in this particular case can yield accurate results at a great saving in computing time.

CASE II—ELASTIC-STRESS DISTRIBUTION IN DISK WITH CENTRAL HOLE

A disk with a central hole is studied in a manner similar to the solid disk except that the first station is taken at the inside boundary instead of at an arbitrary small distance as in the solid disk. The choice of stations near the central hole is, however, critical for this case. Stations should be taken also at distances of 1, 2, 3, and 5 percent of the rim diameter from the inside boundary of the disk. In order to illustrate the procedure, the disk of figure 1 is again used but with a central hole 1 inch in diameter, chosen so that station a will be conveniently located in the same place as station a for Case I.

Columns 1 to 32 for the disk of figure 2 (a) with the central hole are identical to the corresponding columns of table I for the solid disk. In column 33 the entry for station a is 0 instead of 1 as for the solid disk; otherwise, the procedure for calculating columns 33 to 39 is the same as that of table I. Table II gives the modified columns 33 to 39 that result from changing the single first entry in column 33 and figure 5 shows a plot of the resulting radial and tangential stresses; the curves marked "18 stations" are the stress values for this computation.

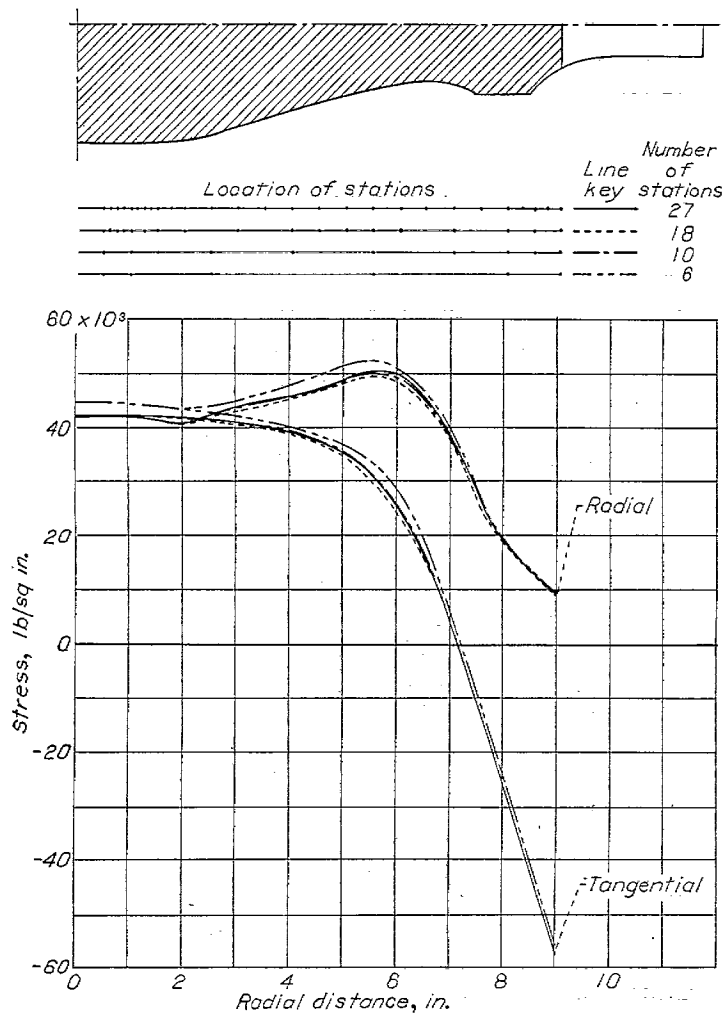


FIGURE 4.—Effect on calculated stress distribution in disk of figure 2 of various numbers of stations.

The results of supplementary calculations using different numbers of stations (fig. 5) indicate that considerable error can result in the determination of the peak stress at the inner boundary if an insufficient number of stations are chosen near this boundary. A more judicious choice of stations for the 6- and 10-station systems could produce more accurate results than those shown; in the absence of experience in choice of locations, however, it is better to choose a large number of stations and insure accuracy.

A practical procedure used to reduce the amount of calculation necessary to obtain the critical end stresses is to calculate the stress distribution on the basis of a solid disk using a few stations and then to modify the stresses in the immediate vicinity of the central hole by the stress-concentration factor characteristically introduced by the hole. A comparison of figures 4 and 5 indicates that, with the exception of the region immediately adjacent to the central hole, the stresses are similar for the cases of the solid disk and of the disk with the central hole; this stress distribution depends very little on the number of stations chosen. By reference 3 (fig. 145), for example, the characteristic stress concentration for a disk with a central hole of which the diameter is one-twentieth of the outside diameter is about 2.0. From calculations based on different numbers of stations, the calculated average stress at the center of the

solid disk (fig. 4) is 43,000 pounds per square inch. The tangential stress at the inside boundary for the disk with the central hole should therefore be $2 \times 43,000 = 86,000$ pounds per square inch. The radial stress at a free boundary is,

TABLE II.—CALCULATION OF STRESSES IN DISK WITH 1-INCH CENTRAL HOLE

[Engine speed, 11,500 rpm; operating temperature, 1270° F at rim, 670° F at center]

	32	33	34	35	36	37	38	39
n	M_n^n $\frac{(20) \times (14) + (8) \times (25)}{(20) \times (25) + (8) \times (14)}$	A_n^n $\frac{(27) \times (33)_{n-1} + (28) \times (34)_{n-1}}{(27) \times (33)_{n-1} + (28) \times (34)_{n-1}}$	A_n^n $\frac{(29) \times (33)_{n-1} + (30) \times (34)_{n-1}}{(29) \times (33)_{n-1} + (30) \times (34)_{n-1}}$	B_n^n $\frac{(27) \times (35)_{n-1} + (28) \times (36)_{n-1} + (31)}{(27) \times (35)_{n-1} + (28) \times (36)_{n-1} + (31)}$	R_n^n $\frac{(29) \times (35)_{n-1} + (30) \times (36)_{n-1} + (32)}{(29) \times (35)_{n-1} + (30) \times (36)_{n-1} + (32)}$	$\sigma_{r,b}^n$ $\frac{(35) \times (37) + (33) \times (38)}{(35) \times (37) + (33) \times (38)}$	$\sigma_{t,b}^n$ $\frac{(33) \times (37) + (35) \times (38)}{(33) \times (37) + (35) \times (38)}$	$\sigma_{t,b}^n$ $\frac{(34) \times (37) + (36) \times (38)}{(34) \times (37) + (36) \times (38)}$
2		0	1.00000			0	85,068	
3		0.18098	0.80981			15,618	70,157	
4		.27748	.71008			23,905	61,474	
5		.33507	.65110			28,808	56,314	
6		.37222	.61330			31,928	52,930	
7		.41585	.58746			35,469	48,867	
8		.43912	.56432			37,195	46,810	
9		.46208	.54358			38,411	43,797	
10		.48705	.52573			42,186	41,797	
11		.51976	.50345			44,818	39,705	
12		.57479	.59041			40,365	37,629	
13		.73691	.62339			47,094	35,002	
14		.81907	.66319			49,525	31,113	
15		.86439	.69322			48,296	25,155	
16		.86126	.70918			38,471	4,844	
17		.67632	.63141			18,990	-26,188	
18		.76229	.64940			13,884	-41,968	
19		.93917	.70575			8,500	-57,028	
b								

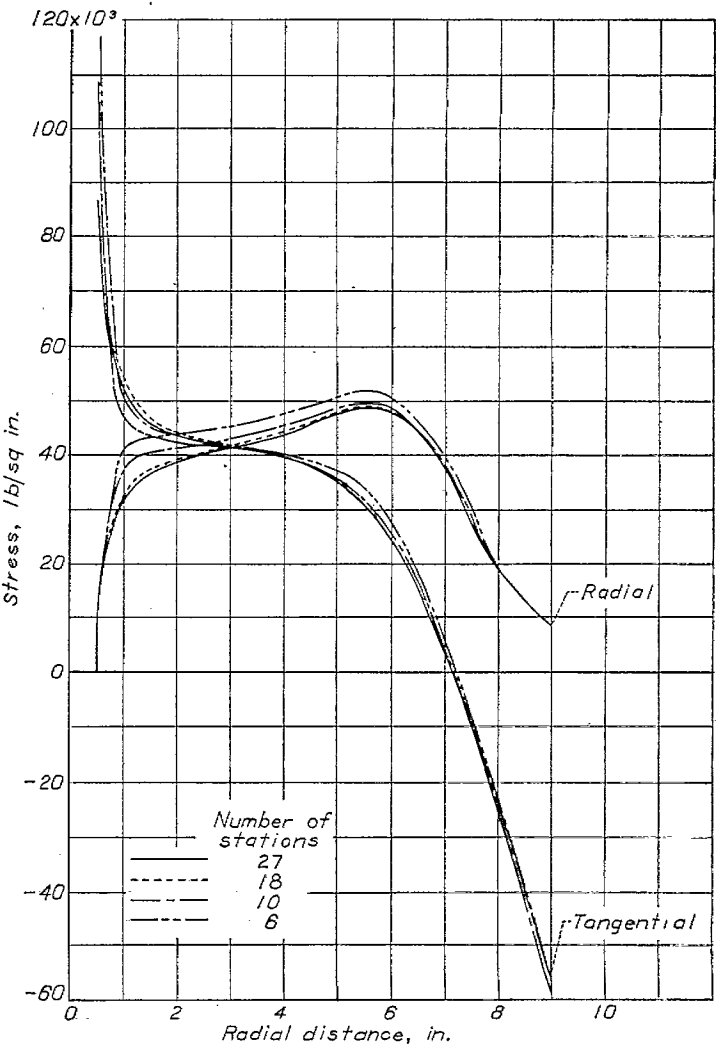


FIGURE 5.—Effect on calculated stress distribution in disk of figure 2 with central hole of various numbers of stations. (Location of stations shown on fig. 4.)

of course, zero. A curve faired between these boundary values and the general curves of figure 4 would coincide very closely with the 27-station result of figure 5.

CASE III—ELASTIC-STRESS DISTRIBUTION IN COMPOSITE WELDED DISKS

For some applications, turbine wheels must be fabricated by welding parts composed of several materials. The method of analysis presented is applicable to studies of composite welded disks in which various alternatives of boundary location and shrink interference can be investigated with few changes in the tabulated computations. The procedure is illustrated for a typical application in which the boundary location is constant.

The disk of figure 2 (a) is assumed to be made in two parts with the boundary at the 6-inch station. Figure 6 shows the two portions of the disk just before welding. The heat-resisting outer portion is heated to 670° F while the inner portion is maintained at 70° F. (In practice both portions may be heated while maintaining a desired temperature differential.) At this temperature condition, an exact fit exists between the mating tips of the two parts. The wedge is then filled with weld metal.

The assumption is made that this temperature differential between the two portions of the disk is maintained throughout the welding process in making the calculations. Any cooling of the outer region prior to the placement of the weld metal would produce a crushing of the mating tips and reduce the effective amount of shrink. Localized effects of the weld metal in producing residual stresses are neglected. The calculations are made as if the high-temperature alloy, having full width at the mating face, is shrunk at 670° F onto the full-width steel central portion. Table III shows the essential tabulations for this case.

In order to insure accuracy, a few more stations than were used in tables I and II have been chosen in the vicinity of the boundary. The densities of the two materials are somewhat different. The quantities for μ and E are the values at the temperatures of figure 2 (b). The quantity ΔT at each station is the difference between the existing temperature and the temperature at which there is zero thermal stress. The temperatures of zero thermal stress occur just before the shrink fit when the outer portion is at 670° F and the inner portion is at 70° F. Therefore, for the outer portion 670° F is subtracted at each station from the temperatures of figure 2 (b) and for the inner portion 70° F is subtracted. The value of α at each station must be the average α between the stress-free temperature and the operating temperature. At the rim, for example, an average coefficient of expansion between 670° and 1270° F must be used. The average temperature coefficient α_{1-2} applicable to the range between any two temperatures T_1 and T_2 can be found by

$$\alpha_{1-2} = \frac{\alpha'_2 T'_2 - \alpha'_1 T'_1}{(T_2 - T_1)(1 + \alpha'_1 T'_1)}$$

where α'_1 and α'_2 are the average coefficients of thermal expansion between room temperature and the temperatures T_1 and T_2 , respectively, and T'_1 and T'_2 are the temperature differences between T_1 and T_2 and room temperature.

The procedure of calculating table III from column 8 on is similar to that of table I. The final calculated values of stress are shown in figure 6.

Comparison of figures 5 and 6 shows that a shrink fit, unless excessive, can have beneficial effects. The shrink fit reduces the tangential tensile stresses that exist near the central hole under operating conditions and also the tangential compressive stress at the rim. Compressive stresses at the rim can be detrimental. If the elastic compressive stresses exceed the yield strength of the material, plastic flow takes place and a residual tangential tensile stress exists after

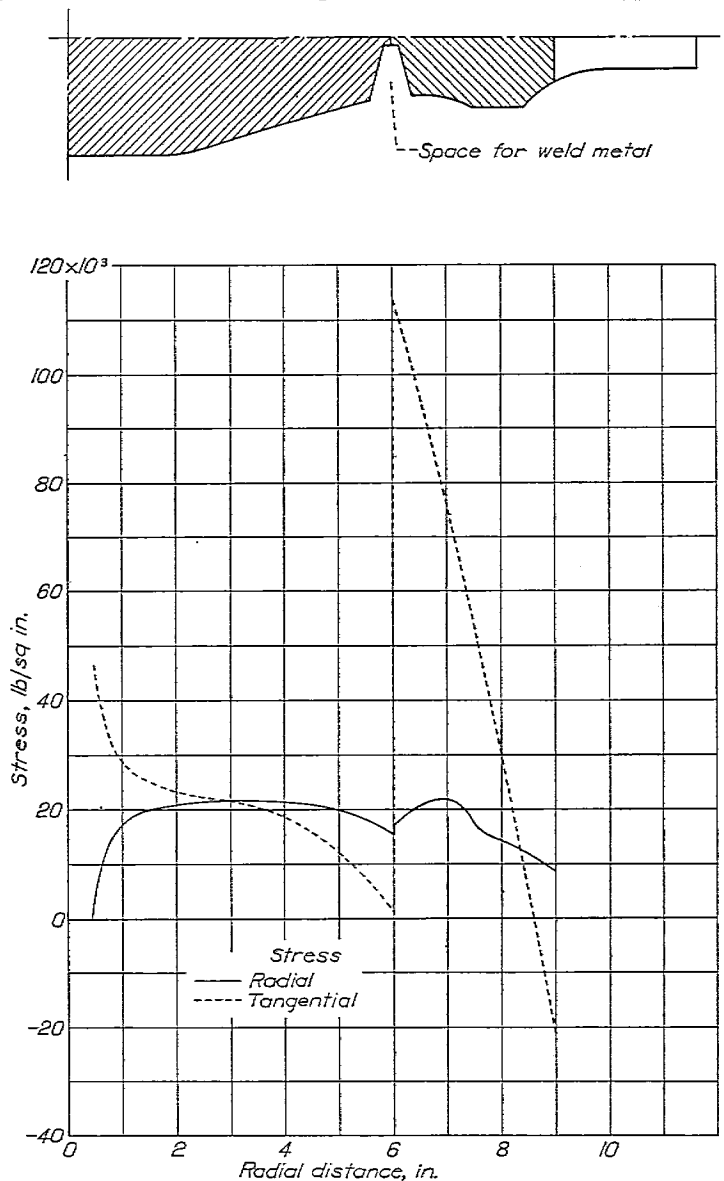


FIGURE 6.—Stresses at running conditions of speed and temperature in composite welded disk. Temperature of operating rim section during welding, 670° F; temperature of central section, 70° F.

operation. Because the region of the rim is a stress-concentrated area as a result of the blade attachments, even relatively small residual tensile stress may cause cracks. The shrink fit removes the high tensile stress at the center and the high compressive stress at the rim but introduces a high tensile stress at the boundary of the two fitted regions. The boundary is at a lower running temperature and has no stress-concentrating effects of the blade attachments.

The optimum amount of shrink, however, is fairly critical. Probably the shrink of the illustrative example is excessive.

TABLE III.—CALCULATION OF STRESSES IN SHRUNK DISK

[Engine speed, 11,500 rpm; operating temperature, 1270° F at rim, 670° F at center; shrinking condition, 670° F for rim portion, 70° F for central portion]

	1	2	3	4	5	6	7	8	9	10	11	12	13	14	15	16	17	18	19	20
r	r_n	h_n	$\rho_n \omega^2$	μ_n	E_n	α_n	ΔT_n	C_n (1) \times (2)	$\frac{(1) - (17)}{(1) + (17)}$	D_n (2) \times (6)	G_n (2) \times (9)	$(3) \times (11)$	$(12) + (12)_{n-1}$	H_n (9) \times (13)	$1 \div (5)$	$(4) \times (16)$	$(1) + (4) \times (16) + (17)$	$(17) \times (10)$	$(17) \times$ (9)	C_n (16) \times (18)
a	0.500	4.375	964.97	0.344	26.0×10^6	7.061×10^{-6}	600	2.1875	0.0625	0.27344	0.27344	1.055.43	2,704.56	169.04	0.088462×10^{-6}	0.013231×10^{-6}	0.103386×10^{-6}	0.005169×10^{-6}	0.006462×10^{-6}	0.018400×10^{-6}
2	0.625	4.375	964.97	0.344	26.0	7.061	600	2.7344	0.0625	0.27344	0.27344	1,049.13	2,704.56	169.04	0.088462	0.013231	0.082709	0.004308	0.005169	0.017589
3	0.750	4.375	964.97	0.344	26.0	7.061	600	3.2813	0.0625	0.27344	0.27344	2,374.79	4,023.92	251.50	0.088462	0.013231	0.068924	0.004308	0.005169	0.016923
4	0.875	4.375	964.97	0.344	26.0	7.061	600	3.8281	0.0625	0.27344	0.27344	3,232.20	5,607.05	350.44	0.088462	0.013231	0.059078	0.004308	0.005169	0.016462
5	1.000	4.375	964.97	0.344	26.0	7.061	600	4.3750	0.0625	0.27344	0.27344	4,221.74	7,464.00	465.88	0.088462	0.013231	0.051693	0.004308	0.005169	0.016103
6	1.125	4.375	964.97	0.344	26.0	7.061	600	4.9219	0.0625	0.27344	0.27344	5,343.14	9,504.88	597.80	0.088462	0.013231	0.045949	0.004308	0.005169	0.015816
7	1.250	4.375	964.97	0.344	26.0	7.061	600	5.4898	0.0625	0.27344	0.27344	6,596.53	11,939.7	746.23	0.088462	0.013231	0.041354	0.004308	0.005169	0.015581
8	1.375	4.375	964.97	0.344	26.0	7.061	600	6.0156	0.0625	0.27344	0.27344	7,981.75	14,578.8	911.14	0.088462	0.013231	0.037595	0.004308	0.005169	0.015385
9	1.500	4.375	964.97	0.344	26.0	7.061	600	6.5025	0.0625	0.27344	0.27344	9,498.97	17,480.7	1,092.5	0.088462	0.013231	0.034402	0.004308	0.005169	0.015164
10	1.750	4.375	964.97	0.344	26.0	7.061	600	7.5663	0.0625	0.27344	0.27344	12,929.0	22,428.6	1,403.6	0.088462	0.013231	0.029539	0.004308	0.005169	0.014800
11	2.000	4.375	964.97	0.344	26.0	7.061	600	8.7500	0.0625	0.27344	0.27344	16,887.0	29,816.6	1,727.1	0.088462	0.013231	0.025846	0.004308	0.005169	0.014384
12	2.500	4.090	964.97	0.344	26.0	7.061	600	10.2250	0.0625	0.27344	0.27344	24,667.5	41,554.5	2,389.9	0.088462	0.013231	0.020677	0.004308	0.005169	0.013840
13	3.000	3.840	964.97	0.344	25.9	7.061	600	12.5200	0.0625	0.27344	0.27344	33,494.4	53,016.9	3,160.4	0.088462	0.013231	0.017297	0.004308	0.005169	0.013276
14	3.500	3.575	964.97	0.344	25.8	7.061	600	15.3550	0.0625	0.27344	0.27344	44,728.4	75,077.6	4,176.9	0.088462	0.013231	0.014895	0.004308	0.005169	0.012596
15	4.000	3.275	964.97	0.344	25.7	7.061	600	18.1000	0.0625	0.27344	0.27344	59,564.4	92,292.6	5,392.6	0.088462	0.013231	0.013093	0.004308	0.005169	0.011706
16	4.500	2.970	964.97	0.344	25.6	7.061	600	21.3850	0.0625	0.27344	0.27344	78,036.2	108,601	6,861.0	0.088462	0.013231	0.011692	0.004308	0.005169	0.010644
17	5.000	2.680	964.97	0.344	25.4	7.061	600	25.0000	0.0625	0.27344	0.27344	104,653.0	122,689	8,869.0	0.088462	0.013231	0.010614	0.004308	0.005169	0.009585
18	5.500	2.372	964.97	0.344	25.0	7.061	600	29.0000	0.0625	0.27344	0.27344	133,892	133,892	11,333.3	0.088462	0.013231	0.0098182	0.004308	0.005169	0.008585
19	5.875	2.240	964.97	0.352	24.6	7.287	709	33.160	0.0625	0.27344	0.27344	163,406.6	143,846	13,471.0	0.088462	0.013231	0.0093547	0.004308	0.005169	0.007898
20	6.000	2.210	1030.21	0.410	26.7	7.981	118	38.260	0.0625	0.27344	0.27344	181,963.5	166,870	15,755.6	0.088462	0.013231	0.0088015	0.004308	0.005169	0.007374
21	6.125	2.190	1030.21	0.410	26.6	8.002	129	43.414	0.0625	0.27344	0.27344	202,797	181,963.5	17,858.0	0.088462	0.013231	0.00825168	0.004308	0.005169	0.006899
22	6.500	2.160	1030.21	0.410	26.4	8.055	163	48.040	0.0625	0.27344	0.27344	220,797	202,797	19,999.0	0.088462	0.013231	0.0077771	0.004308	0.005169	0.006462
23	7.000	2.155	1030.21	0.410	25.9	8.127	220	53.085	0.0625	0.27344	0.27344	240,797	220,797	22,222.2	0.088462	0.013231	0.0073379	0.004308	0.005169	0.006078
24	7.500	2.145	1030.21	0.410	25.3	8.231	280	58.000	0.0625	0.27344	0.27344	260,797	240,797	24,444.4	0.088462	0.013231	0.0069015	0.004308	0.005169	0.005729
25	8.000	2.130	1030.21	0.410	24.5	8.389	375	63.000	0.0625	0.27344	0.27344	280,797	260,797	26,666.7	0.088462	0.013231	0.0064621	0.004308	0.005169	0.005384
26	8.250	2.110	1030.21	0.410	24.1	8.470	424	67.500	0.0625	0.27344	0.27344	300,797	280,797	28,888.9	0.088462	0.013231	0.0060236	0.004308	0.005169	0.005039
27	8.500	2.090	1030.21	0.410	23.5	8.570	477	72.000	0.0625	0.27344	0.27344	320,797	300,797	31,111.1	0.088462	0.013231	0.0055851	0.004308	0.005169	0.004694
28	8.750	2.145	1030.21	0.410	22.9	8.678	536	76.500	0.0625	0.27344	0.27344	340,797	320,797	33,333.3	0.088462	0.013231	0.0051466	0.004308	0.005169	0.004349
b	9.000	1.910	1030.21	0.410	22.1	8.800	600	81.000	0.0625	0.27344	0.27344	360,797	340,797	35,555.6	0.088462	0.013231	0.0047081	0.004308	0.005169	0.004004
21	D_n (16) \times (18)																			
22	F_n (16) \times (19)																			
23	G_n (16) \times (19)																			
24	H_n (16) \times (19)																			
25	I_n (16) \times (19)																			
26	J_n (16) \times (19)																			
27	K_n (16) \times (19)																			
28	L_n (16) \times (19)																			
29	M_n (16) \times (19)																			
30	N_n (16) \times (19)																			
31	O_n (16) \times (19)																			
32	P_n (16) \times (19)																			
33	Q_n (16) \times (19)																			
34	R_n (16) \times (19)																			
35	S_n (16) \times (19)																			
36	T_n (16) \times (19)																			
37	U_n (16) \times (19)																			
38	V_n (16) \times (19)																			
39	W_n (16) \times (19)																			
21	0.48631 $\times 10^{-6}$	0.008769 $\times 10^{-6}$	0.032000 $\times 10^{-6}$	4.238.60 $\times 10^{-6}$	0.00 $\times 10^{-6}$	0.11427 $\times 10^{-6}$	0.81904	0.18098	0.19028	0.80977	64.548	27.219	0.18098	0.80977	64.548	27.219	0.18098	0.80977	64.548	27.219
22	0.42770	0.008032	0.03293	4.238.60	0.00	0.13555	84.13	1.6344	0.18098	0.81331	79.855	32.542	0.18098	0.81331	79.855	32.542	0.18098	0.81331	79.855	32.542
23	0.42154	0.008923	0.03154	4.238.60	0.00	0.15674	86.691	1.3312	0.18098	0.86631	94.248	37.836	0.18098	0.86631	94.248	37.836	0.18098	0.86631	94.248	37.836
24	0.41693	0.009539	0.034770	4.238.60	0.00	0.17790	88.250	1.1753	0.18098	0.88250	100.18	43.110	0.18098	0.88250	100.18	43.110	0.18098	0.88250	100.18	43.110
25	0.41334	0.010000	0.035231	4.238.60	0.00	0.19904	89.430	1.0518	0.18098	0.89430	124.14	48.304	0.18098	0.89430	124.14	48.304	0.18098	0.89430	124.14	48.304
26	0.41047	0.010359	0.035690	4.238.60	0.00	0.22015	90.432	0.95188	0.18098	0.90432	139.13	53.611	0.18098	0.90432	139.13	53.611	0.18098	0.90432	139.13	53.611
27	0.40812	0.010848	0.035877	4.238.60	0.00	0.24125	91.308	0.83922	0.18098	0.91308	154.14	58.845	0.18098	0.91308	154.14	58.845	0.18098	0.91308	154.14	58.845
28	0.40616	0.010881	0.036112	4.238.60	0.00	0.26234	92.000	0.79974	0.18098	0.92000	169.15	64.072	0.18098	0.92000	169.15	64.072	0.18098	0.92000	169.15	64.072
29	0.42154	0.008923	0.034154	4.238.60	0.00	0.28343	92.687	0.73634	0.18098	0.92687	184.16	69.306	0.18098	0.92687	184.16	69.306	0.18098	0.92687	184.16	69.306
30	0.41693	0.009539	0.034770	4.238.60																

There is no need to reduce the stresses at the hole and at the rim as much as shown in figure 6 at the expense of such a high stress at the boundary. An additional calculation can readily be made by using a smaller temperature difference of shrinking than assumed in this calculation. Only columns 6, 7, 24, 31, 32, and 35 to 39 are affected by any change, and the redistribution of stress can be calculated very rapidly. Thus, a more suitable shrink fit can readily be found.

CASE IV—CHECK ON ADEQUACY OF METHOD

Checks on the adequacy of the method were obtained by comparing the results of finite-difference calculations to theoretically correct results in several cases where the latter could be obtained. In one case a parallel-sided disk was studied. The conditions of operation are shown in figure 7;

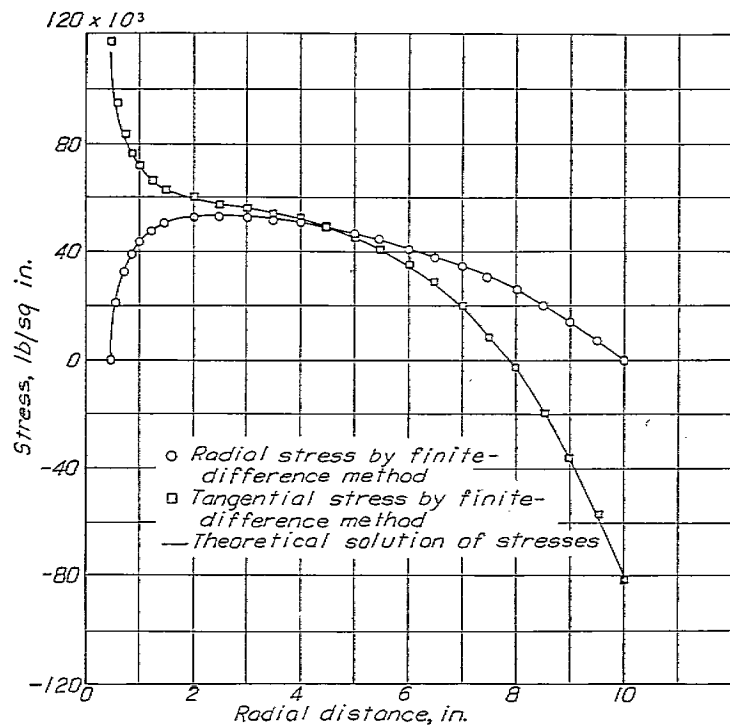


FIGURE 7.—Comparison between theoretical and finite-difference-solution stresses in parallel-sided disk of 20-inch diameter rotating at 10,000 rpm with temperature gradient that varies as fourth power of radius from 600° F at center to 1200° F at rim. E , 30×10^6 pounds per square inch; α , 8×10^{-6} (in./in.)(°F); μ , 0.3.

the circles and squares show the radial and tangential stresses as determined by the finite-difference method, respectively; and the solid lines show the theoretically correct stresses obtained by rigorous solution of equations (1) and (7) for this case in which E , α , and μ are constant. This correlation is seen to be very good. The maximum deviation occurs at the boundary of the central hole where the difference between the tangential stress as computed by the finite-difference method and the theoretically correct value is about 2 percent. The average deviation between the theoretical and finite-difference stresses throughout the disk is less than $\pm \frac{1}{2}$ percent. Checks on a solid disk produced closer agreement, even when a small number of stations was used. A check on a disk of uniform strength produced results differing from the exact solution in the order of $\pm \frac{1}{4}$ percent of the theoretical stresses throughout the entire disk.

CONCLUSIONS

The finite-difference method of calculating stresses in rotating disks has been applied extensively to various types of turbine disk under different conditions of constant temperature or with a temperature gradient. The procedure was found to be convenient and rapid. Where checks were available, the results showed a high degree of accuracy.

FLIGHT PROPULSION RESEARCH LABORATORY,
NATIONAL ADVISORY COMMITTEE FOR AERONAUTICS,
CLEVELAND, OHIO, February 27, 1947.

REFERENCES

1. Thompson, A. Stanley: Stresses in Rotating Disks at High Temperatures. *Jour. Appl. Mech.*, vol. 13, no. 1, March 1946, pp. A45-A52.
2. Stodola, A.: *Steam and Gas Turbines*. Vol. I. McGraw-Hill Book Co., Inc., 1927, pp. 374, 398-400. (Reprinted, Peter Smith (New York), 1945.)
3. Timoshenko, S.: *Strength of Materials*. Part II. D. Van Nostrand Co., Inc., 2d ed., 1941, p. 248.